

~~CONFIDENTIAL~~Copy 5
RM E52E21

NACA RM E52E21

JUL 30 1952

~~NACA~~

RESEARCH MEMORANDUM

PRELIMINARY AIR-FLOW AND THRUST CALIBRATIONS OF SEVERAL
CONICAL COOLING-AIR EJECTORS WITH A PRIMARY TO
SECONDARY TEMPERATURE RATIO OF 1.0

I - DIAMETER RATIOS OF 1.21 AND 1.10

By W. K. Greathouse and D. P. Hollister

Lewis Flight Propulsion Laboratory
Cleveland, Ohio

CLASSIFICATION CANCELLED

Authority *NACA Res. Abs.* Date *5-7-14-56*

FOR REFERENCE

By *RA-1.01*
MA-4 6/8/56 See

NOT TO BE TAKEN FROM THIS ROOM

CLASSIFIED DOCUMENT

This material contains information affecting the National Defense of the United States within the meaning of the espionage laws, Title 18, U.S.C., Secs. 793 and 794, the transmission or revelation of which in any manner to an unauthorized person is prohibited by law.

NATIONAL ADVISORY COMMITTEE
FOR AERONAUTICS

WASHINGTON
July 22, 1952

~~CONFIDENTIAL~~

NATIONAL ADVISORY COMMITTEE FOR AERONAUTICS

RESEARCH MEMORANDUM

PRELIMINARY AIR-FLOW AND THRUST CALIBRATIONS OF SEVERAL CONICAL
COOLING-AIR EJECTORS WITH A PRIMARY TO SECONDARY
TEMPERATURE RATIO OF 1.0

I - DIAMETER RATIOS OF 1.21 and 1.10

By W. K. Greathouse and D. P. Hollister

SUMMARY

An investigation of the performance of several conical cooling-air ejectors was made at primary jet pressure ratios from 1 to 10, secondary shroud pressure ratios from 0.60 to 4.00; and primary to secondary temperature ratio of 1.0. Primary air flow, secondary air flow, primary nozzle thrust, and gross ejector thrust were measured. The data are presented in terms of secondary to primary weight-flow ratio and gross ejector to primary nozzle thrust ratio. This phase of the investigation was limited to ejectors having shroud-exit to primary-nozzle-exit diameter ratios of 1.21 and 1.10 with several spacing ratios for each.

The experimental results indicated that for an ejector having a given diameter ratio, the spacing ratio for maximum thrust was considerably less than the spacing ratio for maximum pumping. The smaller-diameter-ratio ejector produced less thrust loss at secondary pressure ratios below 1.00 than did the large-diameter-ratio ejector. The data further indicated that significant losses in gross thrust will occur if the cooling-air flow is controlled by throttling in the upstream secondary flow passage.

INTRODUCTION

The air ejector has been established as a simple, light-weight device for pumping cooling air for turbojet-engine installations and has been the subject of numerous theoretical and experimental investigations. Reference 1 presents conical-ejector design charts and air-flow information for primary total to ambient pressure ratios from 1 to 2.80. Pumping characteristics of cylindrical ejectors in reference 2 and of conical ejectors with zero secondary air flow in reference 3 give ejector performance at the higher pressure ratios that are encountered at high flight speeds. Proper selection of an ejector configuration, however, requires knowledge of the thrust performance at various operating

conditions, as well as of the pumping characteristics presented in the references.

In order to extend the range of existing cooling-air flow data and to make thrust performance data available, the NACA Lewis laboratory is conducting an experimental investigation of conical-type cooling-air ejector models. Experimental results are presented for a limited number of ejector configurations operating over a wide range of conditions; little attempt was made herein to establish optimum ejector design. Thrust and pumping characteristics over a range of primary pressure ratios P_p/p_0 from 1 to 10 and secondary pressure ratios P_s/p_0 to 4.00 are given for conical ejectors having diameter ratios D_s/D_p of 1.21 and 1.10 with spacing ratios S/D_p of approximately 0.4, 0.8, 1.2, and 1.6 for each. The investigation was conducted with a convergent primary jet nozzle and a conical secondary shroud with unheated air at a temperature of approximately 80° F.

APPARATUS

The nomenclature used for the conical-ejector investigations is listed in figure 1 and the apparatus used is schematically shown in figure 2. The ejector consisted of a primary jet nozzle within a concentric shroud extending into an exhaust chamber connected to the laboratory exhaust system. Primary and secondary air flows were introduced into concentric pipes and passed through the ejector into the exhaust chamber. The capacity of the system enabled the total pressure to be varied to a maximum of 72 inches of mercury absolute for the primary and to 56 inches for the secondary, while the exhaust pressure was reduced from atmospheric to 4 inches of mercury absolute. The air was passed through a drier and supplied at 80° F with a humidity of 2 grains of moisture per pound of dry air.

Primary and secondary air flows were measured by means of standard A.S.M.E. sharp-edge orifices. Total pressure and temperatures were measured by total-pressure tubes and iron-constantan thermocouples. The primary and secondary pressure measuring stations were $17\frac{1}{4}$ inches and $4\frac{1}{2}$ inches upstream of the primary nozzle exit, respectively. The primary stream temperature station was $4\frac{3}{4}$ inches upstream of the primary nozzle exit and the secondary temperature station was $4\frac{1}{2}$ inches upstream of the same exit. Exhaust pressure was measured by static pressure taps located on the outside of the shroud-exit lip.

The ejector air supply ducts were connected to the laboratory air system by flexible bellows and pivoted to a steel frame in order to freely transmit the axial force to a balanced-pressure diaphragm, null-type, thrust-measuring cell which produced an output pressure directly

proportional to the applied force. A counterweight was connected to the ejector rig by large pulleys and steel tapes so that an axial preload force could be applied to the thrust cell. The slip joint between the ejector ducts and exhaust chamber had adequate clearance to prevent metal-to-metal contact.

The primary nozzle had a half-cone angle of 8° , an exit diameter of 4 inches, and a 5-inch-inside-diameter approach pipe. The shroud had an 8° half-cone angle and a 10-inch-inside-diameter approach pipe.

PROCEDURE

The performance of each ejector configuration was investigated over a range of primary pressure ratios from 1 to about 10 with various constant secondary pressure ratios up to 4.00. Additional tests were performed for zero secondary air flow with the upstream secondary-flow passage blocked. Also, a calibration of the primary nozzle with the shroud removed was made to determine flow coefficients and primary nozzle thrust over the range of primary pressure ratios.

Two shrouds with different exit diameters were used to provide diameter ratios D_s/D_p of 1.21 and 1.10. The spacing ratio S/D_p was varied for each diameter ratio to values of approximately 0.4, 0.8, 1.2, and 1.6 by inserting spacer rings and gaskets between the approach pipe and the shroud.

The axial force transmitted to the thrust cell was composed of (1) the ejector thrust force, (2) the pressure-area force acting on the ejector which resulted from the pressure differential across the slip joint, and (3) the axial preload force. The pressure-area force was determined from a calibration over the exhaust-pressure range. The preload was kept at such a value that the net force on the thrust cell was always in the same direction. The ejector thrust was obtained by subtracting the force acting on the thrust cell from the sum of the preload and pressure-area forces. In order to assure accurate and consistent thrust data, the pressure-area force calibration curve was checked daily throughout the investigation.

RESULTS AND DISCUSSION

Pumping Characteristics

The effect of primary pressure ratio P_p/p_0 on weight-flow ratio W_s/W_p at various constant secondary pressure ratios P_s/p_0 is shown in figures 3(a) to 3(d) for the 1.21-diameter-ratio ejector and in figures 3(e) to 3(h) for the diameter ratio of 1.10. Figure 3(a) presents

ejector pumping characteristics that are typical of the conical-type configuration in this investigation. The curve intercepts on the P_p/p_0 -axis were determined with the upstream secondary flow passage blocked (zero secondary flow). For secondary pressure ratios less than 1.00, pressure in the secondary shroud was less than exhaust-chamber pressure. Therefore, at low primary pressure ratios, a certain amount of air flowed from the exhaust chamber into the shroud, where it was entrained by the primary jet and discharged. At the lower primary pressure ratio for which the weight-flow ratio was zero, the inflow was exactly balanced by the entrainment. As the primary pressure ratio was increased beyond this point, the ejector pumping action stopped the inflow and so influenced the secondary flow that the weight-flow ratio reached peak values, and then decreased to zero as the primary jet overexpanded into the conical mixing section (reference 1). For secondary pressure ratios greater than 1.00, increasing the primary pressure ratio caused the primary jet to progressively block the secondary flow area until the weight-flow ratio was decreased to zero.

The range of operation at a given secondary pressure ratio was thus limited by the primary pressure ratio at which the secondary flow became zero (hereinafter referred to as the cut-off point). Operation beyond the cut-off point in actual aircraft installations will result in a back flow from the primary jet into the secondary system.

Performance characteristics illustrated in figure 3(d), for the largest diameter and spacing ratio investigated ($D_s/D_p = 1.21$, $S/D_p = 1.58$), were somewhat different from those of other configurations. The regions shown by broken lines were very unstable and data points could not be obtained to determine the exact shape of all the curves. A brief inspection of the static pressure profile along the shroud wall indicated that this phenomenon was caused by a series of multiple shock and expansion waves in this particular configuration.

Another peculiarity in ejector performance is shown in figure 3(e) for the smallest diameter and spacing ratio investigated ($D_s/D_p = 1.10$, $S/D_p = 0.39$). Two distinct regions of peak weight-flow ratio occurred for secondary pressure ratios of both 0.90 and 0.95.

The effect of spacing ratio S/D_p on weight-flow ratio is demonstrated in figure 4 for the diameter ratios of 1.21 and 1.10. These curves are crossplots of preceding figures and are shown for primary pressure ratios of 2.00, 3.50, and 9.00, which may be considered representative of take-off, high subsonic, and supersonic flight conditions, respectively. Except for figure 4(a), these plots indicate the ejector spacing ratio at which maximum weight-flow ratio occurred. For a given diameter ratio, the spacing ratio that provided maximum weight-flow ratio was about the same for all three primary pressure ratios.

Therefore, optimum pumping characteristics may be closely approximated over a range of operating conditions with an ejector having a fixed spacing ratio. Comparison of figures 4(a) to 4(c) and 4(d) to 4(f) reveals that maximum weight-flow ratio generally occurred at a larger spacing ratio for the ejector having the larger diameter ratio, for example, at a spacing ratio of about 1.3 to 1.5 for the diameter ratio of 1.21 and at a spacing ratio of approximately 1.0 for the 1.10 diameter ratio. A final choice of ejector geometry must, however, be based on thrust performance as well as on optimum pumping characteristics.

The primary pressure ratio at which secondary flow became zero (cut-off point) is shown in figure 5 to indicate how variations in spacing ratio affect the range of primary pressure ratios over which the ejector will operate. For secondary pressure ratios less than 1.00, the ejector will pump cooling air over the range of primary pressure ratios contained between the two secondary-pressure-ratio curves. For secondary pressure ratios greater than 1.00, the range of operation is bounded by the vertical axis ($P_p/p_0 = 1.0$) and one secondary-pressure-ratio curve. Four curves are shown for the secondary pressure ratio of 0.90 in figure 5(b) because the ejector did not pump in the cross-hatched region, as may be surmised from figure 3(e). At a particular spacing ratio and secondary pressure ratio above 1.00, the cut-off point occurred at a higher primary pressure ratio for the larger-diameter-ratio ejector, as might be expected, because to fill the shroud of the larger-diameter-ratio ejector a greater primary jet expansion angle (and hence, greater primary pressure ratio) was required.

Thrust Characteristics

The effect of primary pressure ratio on ejector thrust ratio F_{ej}/F_j is shown in figure 6 for several values of constant secondary pressure ratio. Because the thrust ratio is defined as the ratio of gross ejector thrust to gross primary nozzle thrust (without the shroud) at the same over-all primary pressure ratio, values of thrust ratio less than 1.0 denote a loss in jet thrust below that of the convergent primary nozzle alone, and values of thrust ratio greater than 1.0 denote a gain in thrust with the ejector. This method, of course, does not charge either stream for inlet momentum of air flow.

The lines marked X in figure 6 are thrust ratios of the ejector obtained with zero secondary flow (upstream secondary passage blocked) and will be referred to as the zero-flow thrust curve. Characteristics of this curve are similar to those of a convergent-divergent nozzle thrust curve and are discussed in reference 3, along with the effects of shock losses on ejector thrust.

In general, the thrust-ratio curves at constant secondary pressure ratio meet the zero-flow thrust curve at the same primary pressure ratio for which the weight-flow ratio curves of the same configuration became zero. However, for both diameter ratios with the smallest spacing ratio investigated, (figs. 6(a) and 6(e)), several thrust-ratio curves intersected and came below the zero-flow thrust curve at low values of primary pressure ratio. This occurred because at a given over-all primary pressure the effective pressure ratio across the primary nozzle decreased as the pressure in the shroud increased; that is, effective primary pressure ratio approximately equals $\frac{P_p}{P_s} = \frac{P_p/P_0}{P_s/P_0}$. Therefore, at pressure ratios

for which the primary nozzle was not choked, a greater mass flow (and hence, greater thrust) was produced in the primary system at zero-secondary-flow conditions than with a finite secondary air flow and consequent higher shroud pressure.

For a specific ejector configuration, the general trends (at constant secondary pressure ratio) of the thrust-ratio and weight-flow-ratio curves were similar. Ejector thrust ratios both greater and smaller than 1.0 were obtained at high secondary pressure ratios. But at secondary pressure ratios below 1.00, the thrust-ratio curve remained below 1.0 for all configurations. The minimum value of thrust ratio occurred with zero secondary flow for all ejectors investigated and when a relatively small amount of secondary flow was introduced (increased secondary pressure ratio), the thrust ratio greatly increased. Thus, if an ejector were operating at a certain primary pressure ratio with a constant pressure at the inlet of the secondary flow system, a large reduction in gross thrust would occur if the secondary flow were reduced by throttling in the upstream secondary flow passage. For the eight ejector configurations investigated, the magnitude of the maximum thrust loss at zero secondary flow was changed by variations in either the diameter ratio or the spacing ratio. Losses as great as 21.5 and 12 percent of convergent nozzle thrust occurred for the 1.21 and 1.10 diameter ratio ejector, respectively.

The effect of spacing ratio on thrust ratio is shown in figure 7 for the 1.21 and 1.10 diameter ratios. These cross plots of preceding figures are shown for constant secondary pressure ratios and for zero secondary flow at primary pressure ratios of 2.00, 3.50, and 9.00.

For the 1.21-diameter-ratio ejector (figs. 7(a) to 7(c)), changes in spacing ratio at constant secondary pressure ratio had only a moderate effect on thrust ratio, the direction of the effect depending upon the conditions at which the ejector was operating. Maximum thrust ratio, however, generally occurred at a spacing ratio between 0.4 and 0.8. Thus, it is indicated that the spacing ratio for maximum thrust is less than the spacing ratio for maximum pumping ($S/D_p = 1.3$ to 1.5, from

figs. 4(a) and 4(b)). At zero secondary flow, a minimum thrust ratio occurred at a spacing ratio of about 1.20 for the three primary pressure ratios shown.

As shown in figure 7(d) to 7(f) for the 1.10-diameter-ratio ejector, the maximum thrust ratio occurred between spacing ratios of 0.60 and 1.00 for all the constant-secondary-pressure-ratio curves. Therefore, it is again indicated that the spacing ratio for maximum thrust is less than the spacing ratio for maximum pumping ($S/D_p =$ about 1.0, from figs. 4(d) to 4(f)). For zero secondary flow, the minimum thrust ratio occurred at a spacing ratio of about 1.3.

Comparison of the two diameter ratio ejectors at a fixed spacing shows that greater thrust was attained by the large diameter ratio at high secondary pressure ratios, but for low secondary pressure ratios, greater thrust was attained with the small diameter ratio.

The comparisons made herein are based on ejector characteristics alone. For a specific aircraft installation, a final choice of ejector geometry must be based on the combined performance of the ejector and the cooling-air supply ducting over the complete range of operating conditions. Also, it must be remembered that the data presented herein were obtained with an unheated primary jet at an ejector temperature ratio of 1.0. A correction to the values of weight-flow ratio must be made for the ratio of cooling-air to engine-gas temperature (hot weight-flow ratio = cold weight-flow ratio $\times \sqrt{T_p/T_g}$) as described in reference 4. This correction factor, however, is applicable only at relatively low secondary pressure ratios as shown in reference 5.

The exact effect of high temperature on ejector characteristics has not been completely determined. Reference 4, however, showed that a heated primary jet increased the weight-flow ratio, reference 3 indicated a shift in the cut-off point to slightly lower primary pressure ratios, and reference 5 revealed roughly a 5-percent loss in ejector thrust for a temperature ratio of 3.0 as compared with the thrust at a temperature ratio of 1.0. In spite of this somewhat limited evidence, it must be assumed, until more complete high-temperature data are available, that performance of full-scale ejectors operating at temperature ratios greater than 1.0 may be approximated by cold-model-ejector data corrected to the desired temperature ratio.

CONCLUDING REMARKS

The experimental data presented herein showing pumping and thrust characteristics of conical cooling-air ejectors indicated that for each diameter ratio (1.21 and 1.10) there existed a spacing ratio that gave

maximum pumping and another that gave maximum thrust for a particular primary and secondary pressure ratio. The spacing for maximum thrust was shorter than that for maximum pumping.

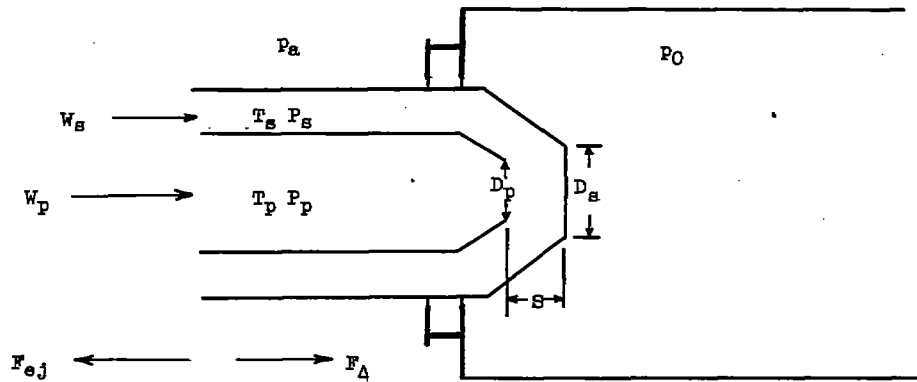
For a given spacing ratio and secondary pressure ratio, the 1.21-diameter-ratio ejector pumped cooling air over a wider range of primary pressure ratios than did the 1.10-diameter-ratio ejector.

At high secondary pressure ratios, both the 1.21- and 1.10-diameter-ratio ejectors produced gross thrust ratios greater than 1.0, but at low secondary pressure ratios the smaller diameter ratio gave the least loss of thrust. At zero secondary flow conditions, thrust losses as great as 21.5 and 12 percent of convergent nozzle thrust occurred for the 1.21- and 1.10 diameter-ratio ejectors, respectively. The data indicated that reducing the cooling-air flow by throttling it upstream of the ejector introduces additional gross thrust losses that become very large at some operating conditions.

Lewis Flight Propulsion Laboratory
National Advisory Committee for Aeronautics
Cleveland, Ohio

REFERENCES

1. Huddleston, S. C., Wilsted, H. D., and Ellis, C. W.: Performance of Several Air Ejectors with Conical Mixing Sections and Small Secondary Flow Rates. NACA RM E8D23, 1948.
2. Kochendorfer, Fred D., and Rousso, Morris D.: Performance Characteristics of Aircraft Cooling Ejectors Having Short Cylindrical Shrouds. NACA RM E51E01, 1951.
3. Ellis, C. W., Hollister, D. P., and Sargent, A. F.: Preliminary Investigation of Cooling-Air-Ejector Performance at Pressure Ratios of from 1 to 10. NACA RM E51H21, 1951.
4. Wilsted, H. D., Huddleston, S. C., and Ellis, C. W.: Effect of Temperature on Performance of Several Ejector Configurations. NACA RM E9E16, 1949.
5. Mickey, F. E.: An Investigation of the Pumping and Thrust Characteristics of a Jet Ejector Operating at High Temperature and Pressure. Rep. ES 21468, Douglas Aircraft Co., Inc. (El Segundo, Calif.) June 24, 1949, (Contract Noa(s) 9517, Phase XI of W.O. 606).



- D_p exit diameter of primary nozzle
 D_s exit diameter of secondary shroud
 F_{ej} gross ejector thrust
 F_j gross thrust of primary nozzle without shroud
 F_A pressure-area force acting on ejector = $(P_a - P_0) \times \text{constant}$
 P_p total primary pressure
 P_s total secondary pressure
 P_a atmospheric pressure
 P_0 ambient or exhaust pressure
 S spacing, distance from primary exit to shroud exit
 T_p total primary temperature, $^{\circ}R$
 T_s total secondary temperature, $^{\circ}R$
 W_p primary weight flow, lb/sec
 W_s secondary weight flow, lb/sec
 D_s/D_p diameter ratio
 F_{ej}/F_j thrust ratio
 P_p/P_0 primary pressure ratio
 P_s/P_0 secondary pressure ratio
 S/D_p spacing ratio
 $\sqrt{T_p/T_s}$ weight-flow correction factor - cold data to hot data
 W_s/W_p weight-flow ratio



Figure 1. - Nomenclature for ejector investigation.

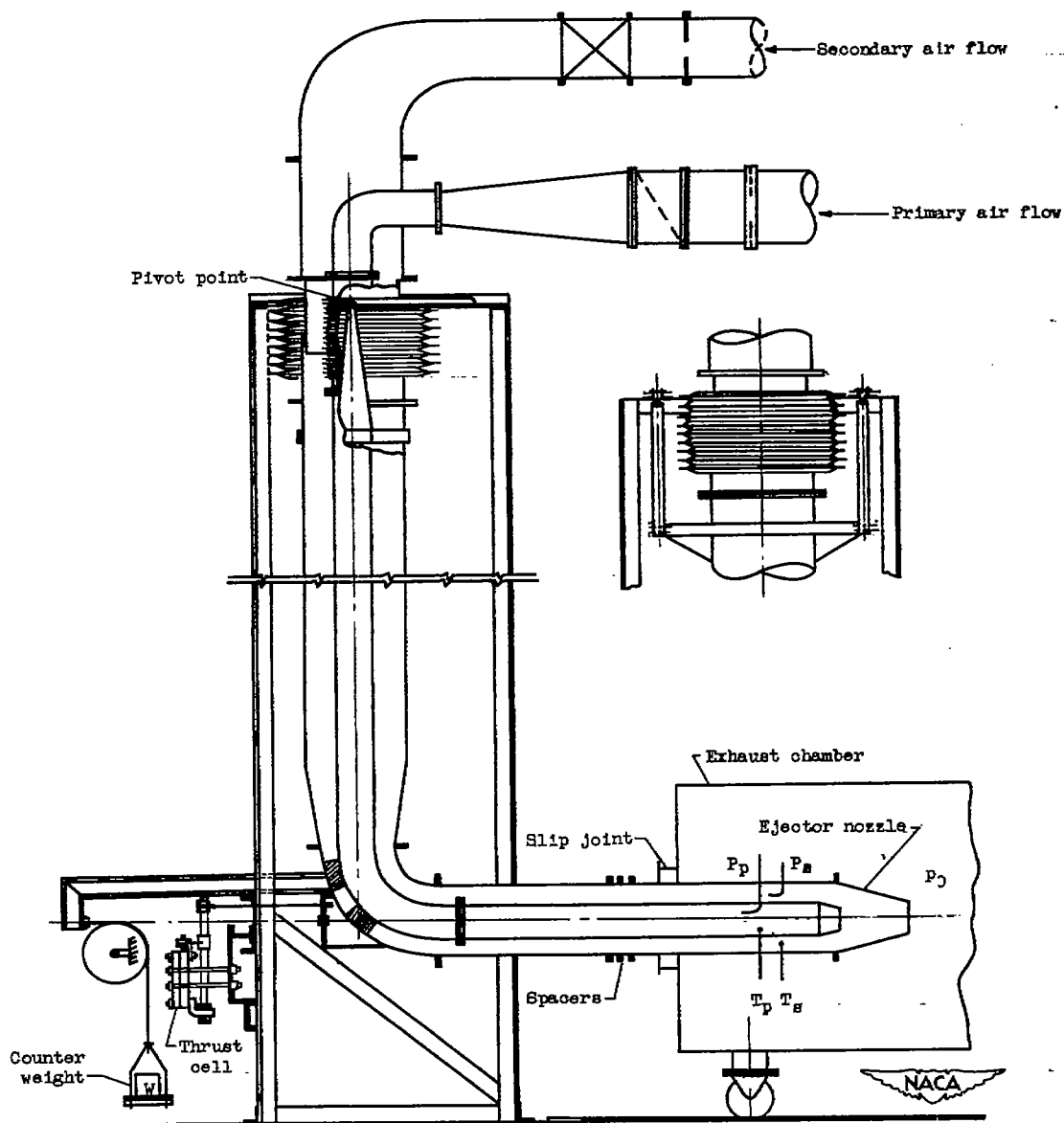
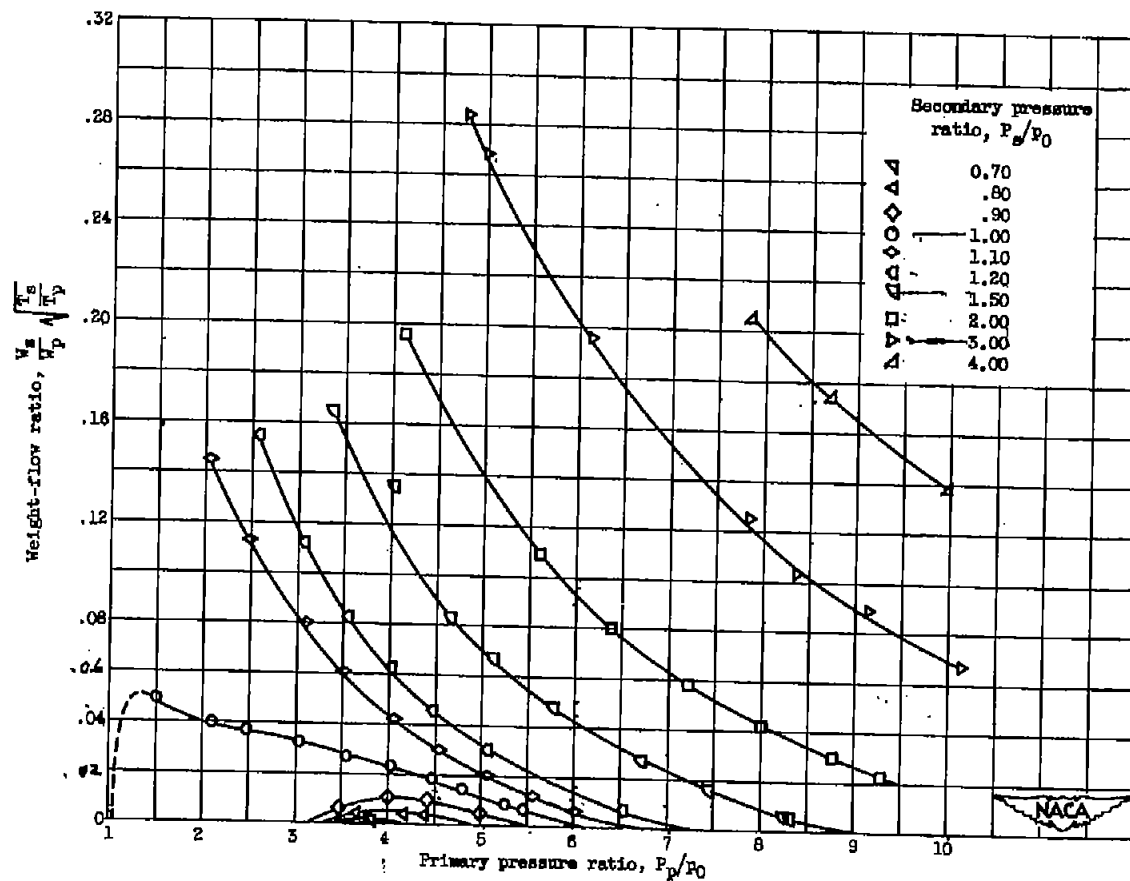
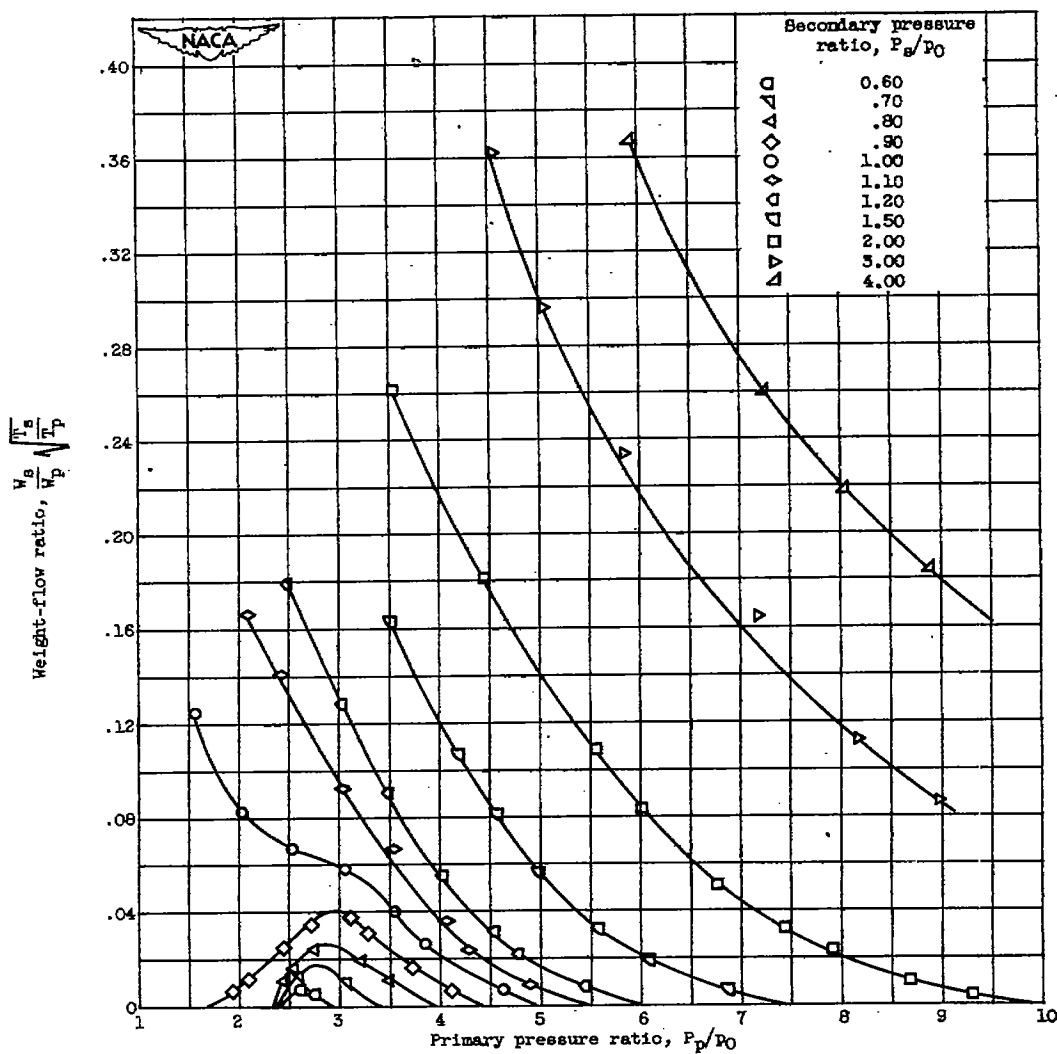


Figure 2. - Schematic diagram of model setup for ejector investigation.



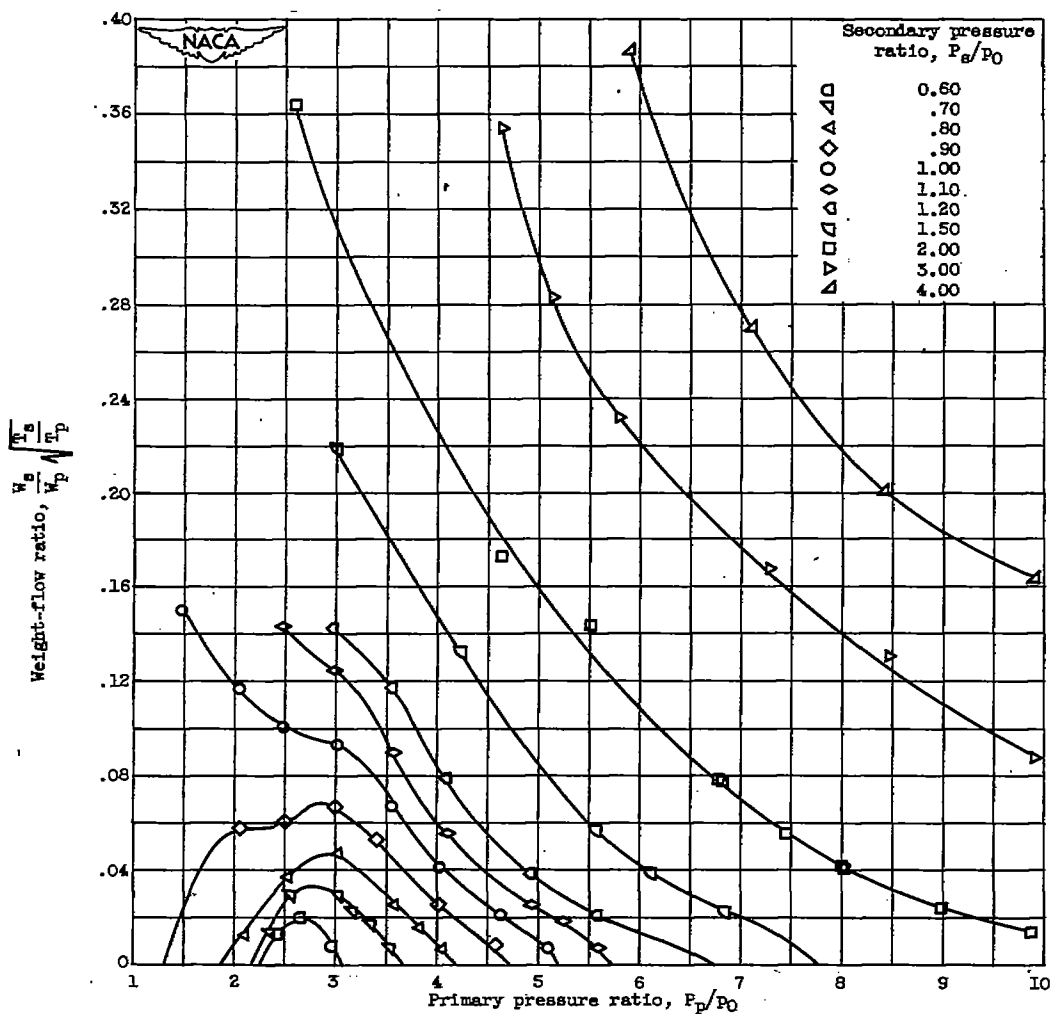
(a) Diameter ratio D_s/D_p , 1.21; spacing ratio S/D_p , 0.59.

Figure 5. - Effect of primary and secondary pressure ratio on ejector weight-flow ratio.



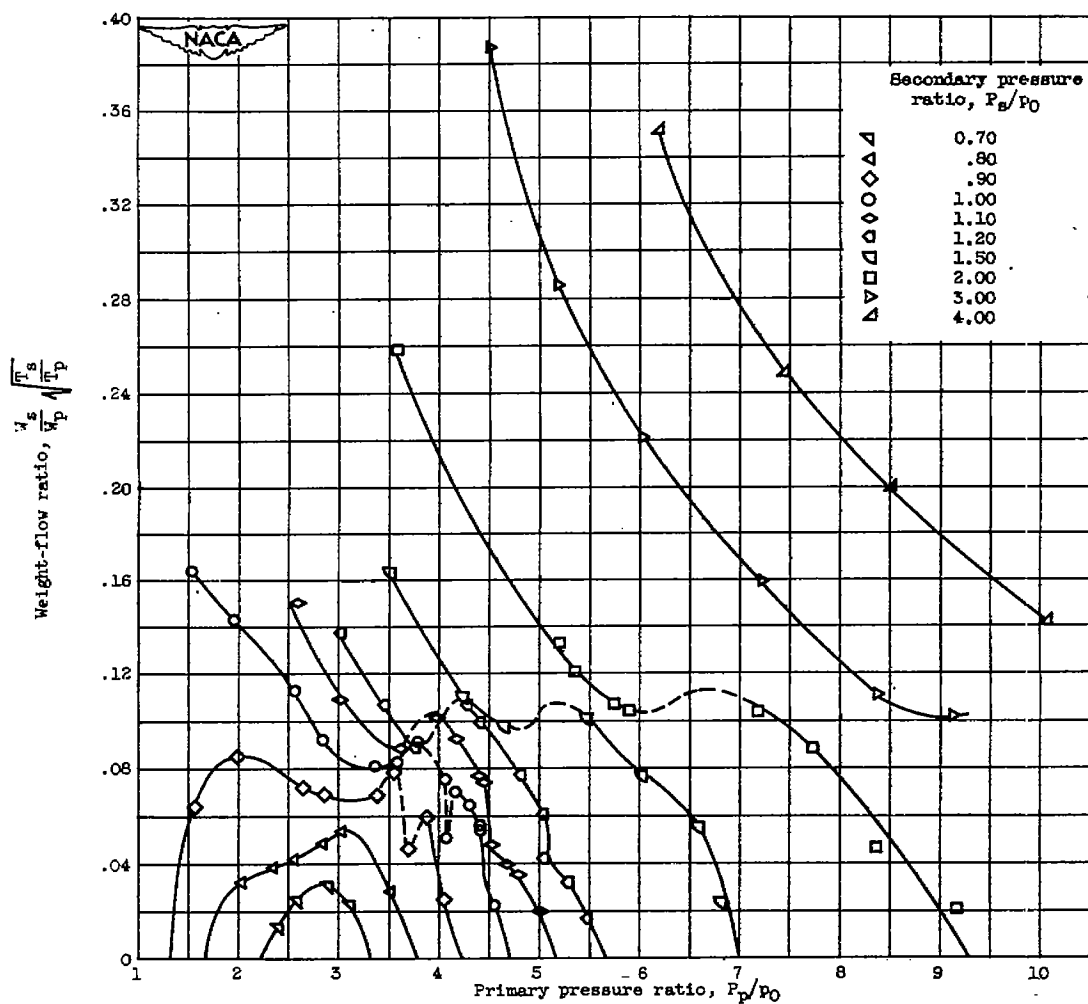
(b) Diameter ratio D_s/D_p , 1.21; spacing ratio S/D_p , 0.79.

Figure 3. - Continued. Effect of primary and secondary pressure ratio on ejector weight-flow ratio.



(c) Diameter ratio D_s/D_p , 1.21; spacing ratio S/D_p , 1.18.

Figure 3. - Continued. Effect of primary and secondary pressure ratio on ejector weight-flow ratio.



(d) Diameter ratio D_s/D_p , 1.21; spacing ratio s/D_p , 1.58.

Figure 3. - Continued. Effect of primary and secondary pressure ratio on ejector weight-flow ratio.

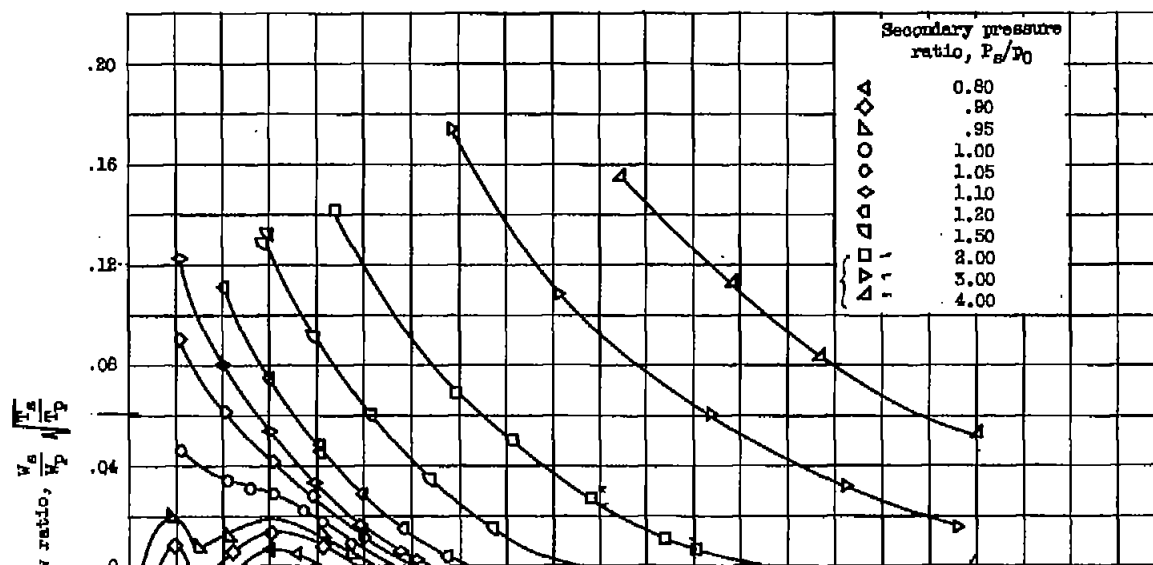
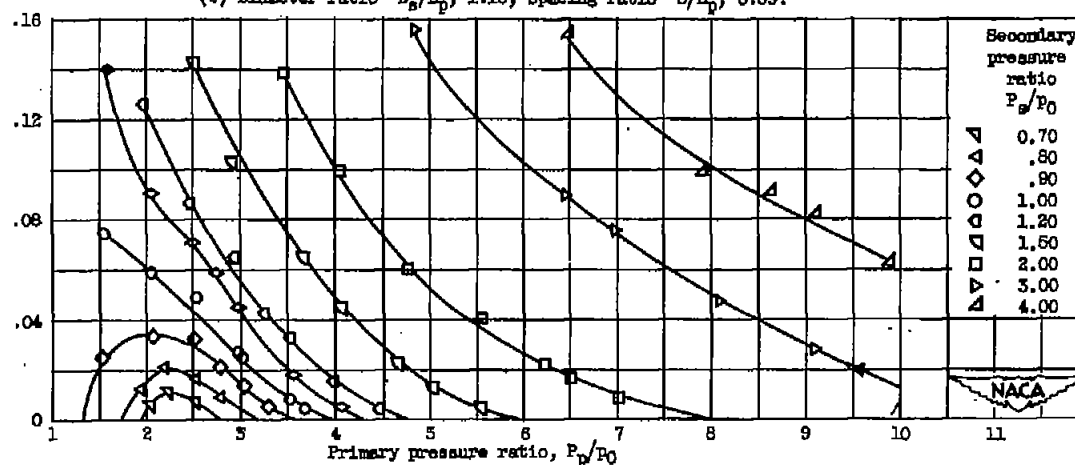
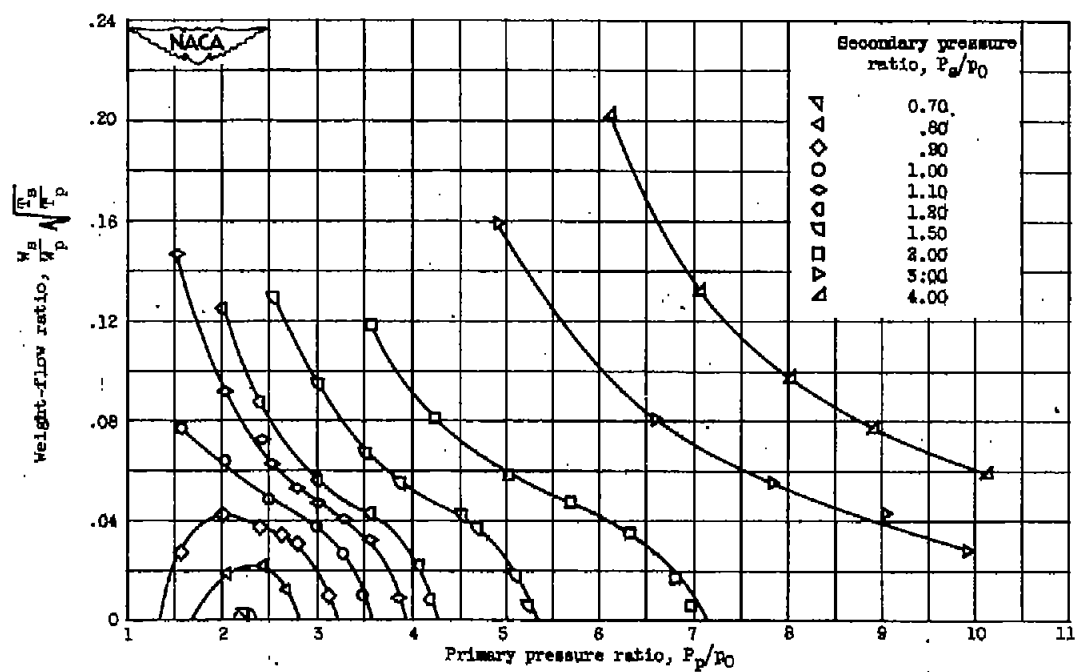
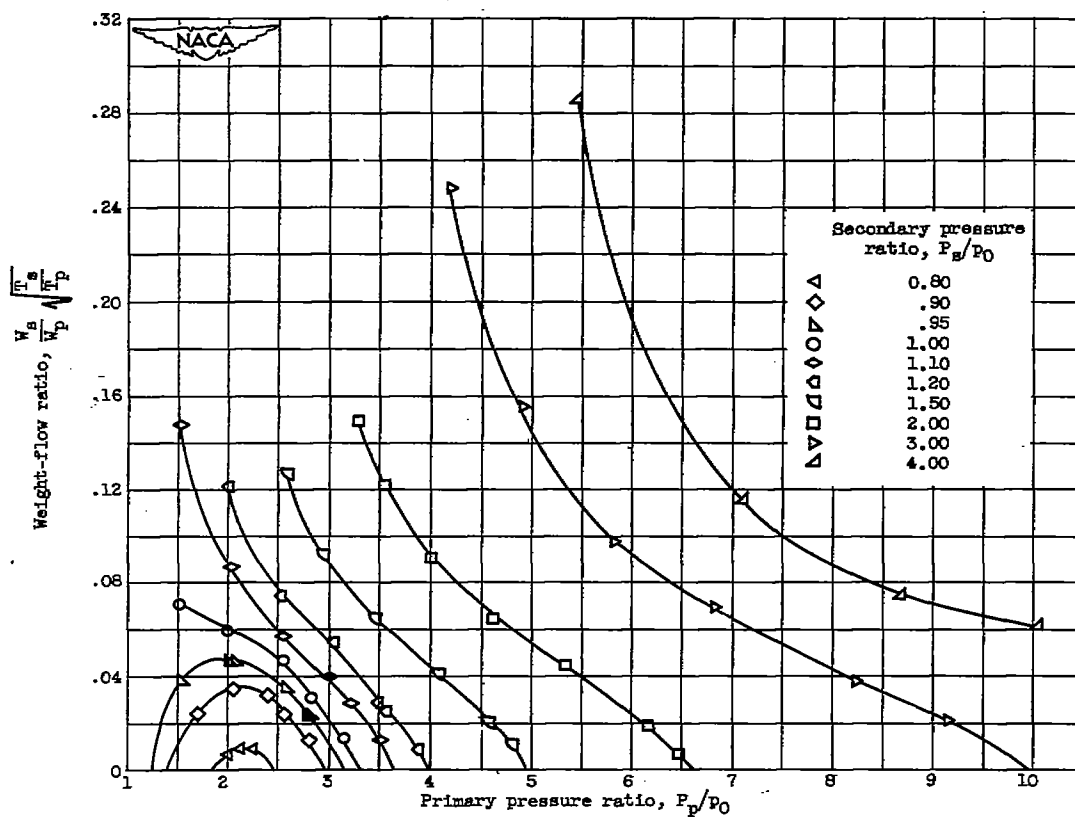
(e) Diameter ratio D_s/D_p , 1.10; spacing ratio S/D_p , 0.39.(f) Diameter ratio D_s/D_p , 1.10; spacing ratio S/D_p , 0.79.

Figure 3. - Continued. Effect of primary and secondary pressure ratio on ejector weight-flow ratio.



(g) Diameter ratio D_s/D_p , 1.10; spacing ratio S/D_p , 1.20.

Figure 3. - Continued. Effect of primary and secondary pressure ratio on ejector weight-flow ratio.



(h) Diameter ratio D_s/D_p , 1.10; spacing ratio S/D_p , 1.61.

Figure 3. - Concluded. Effect of primary and secondary pressure ratio on ejector weight-flow ratio.

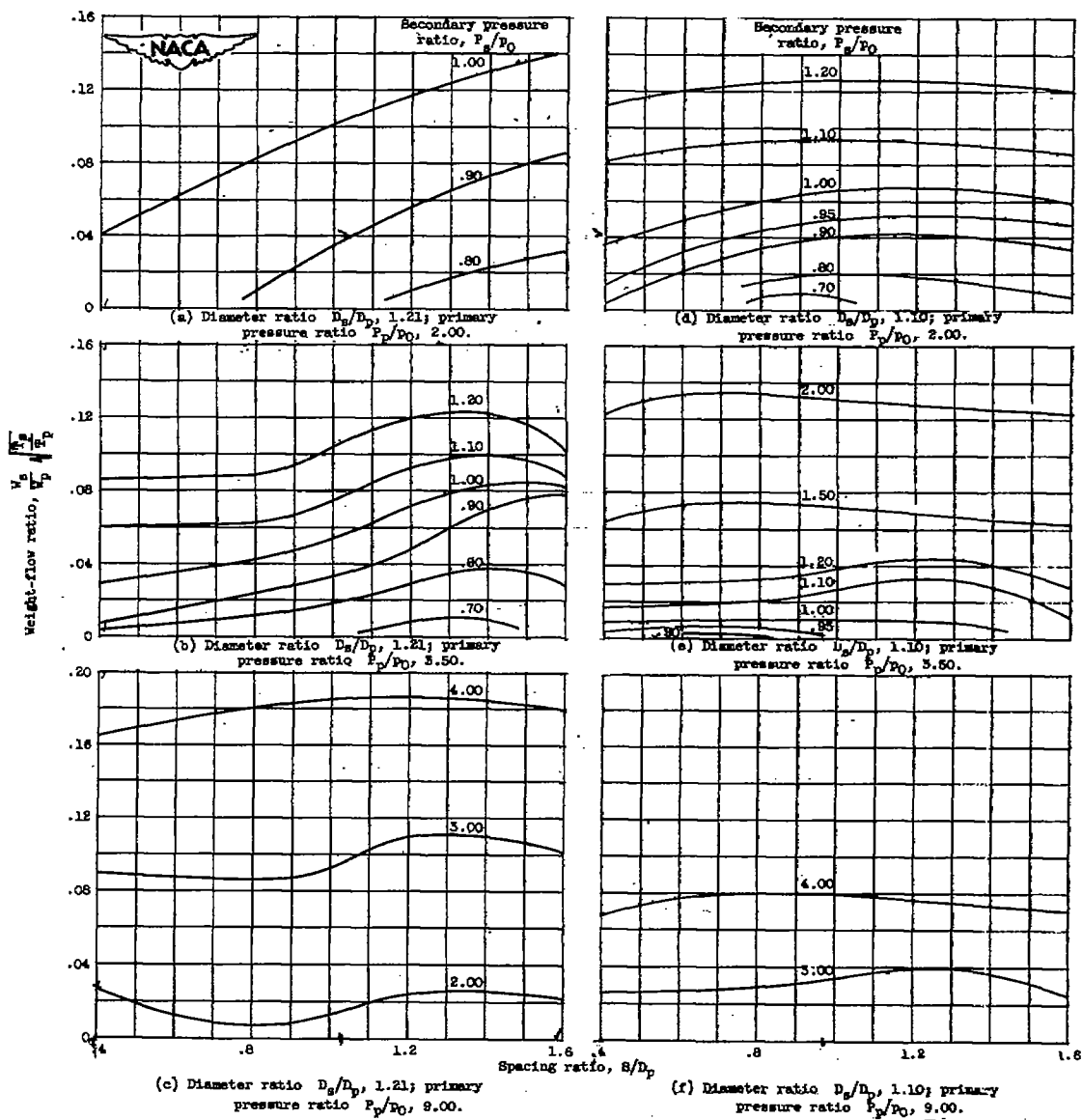


Figure 4. - Effect of spacing ratio on weight-flow ratio.

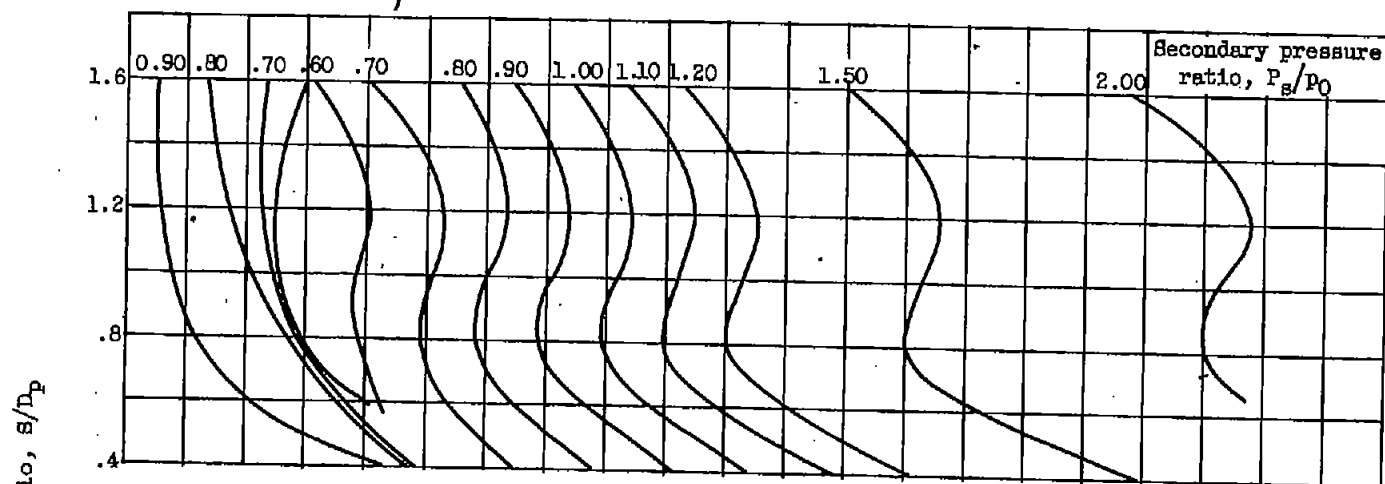
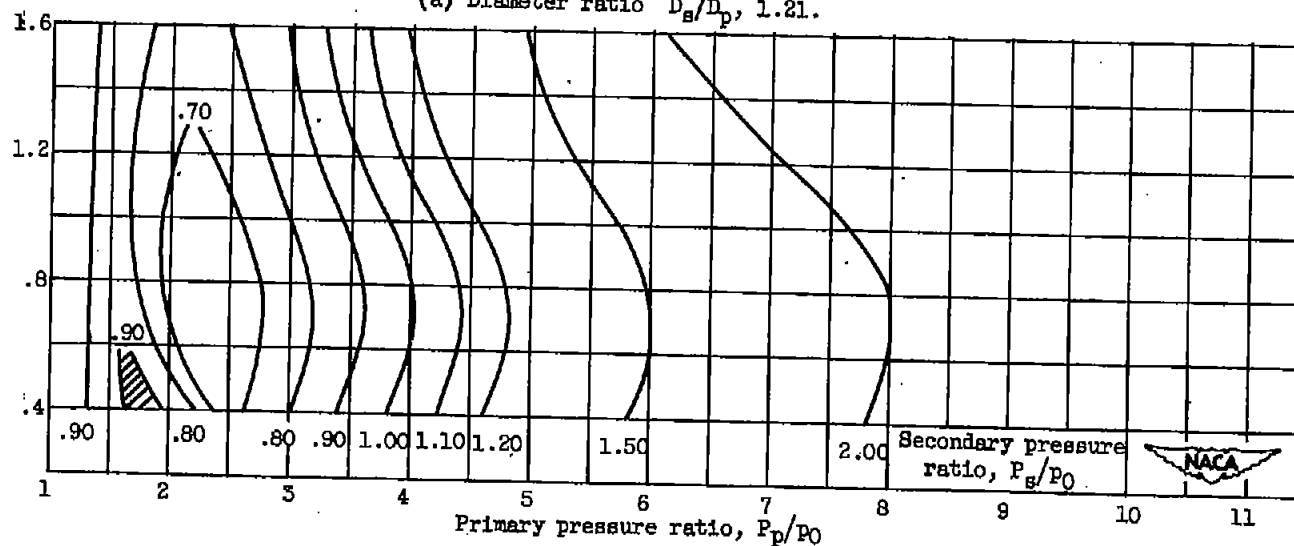
(a) Diameter ratio D_s/D_p , 1.21.(b) Diameter ratio D_s/D_p , 1.10.

Figure 5. - Effect of spacing ratio on the primary pressure ratio at which zero secondary weight-flow occurs.

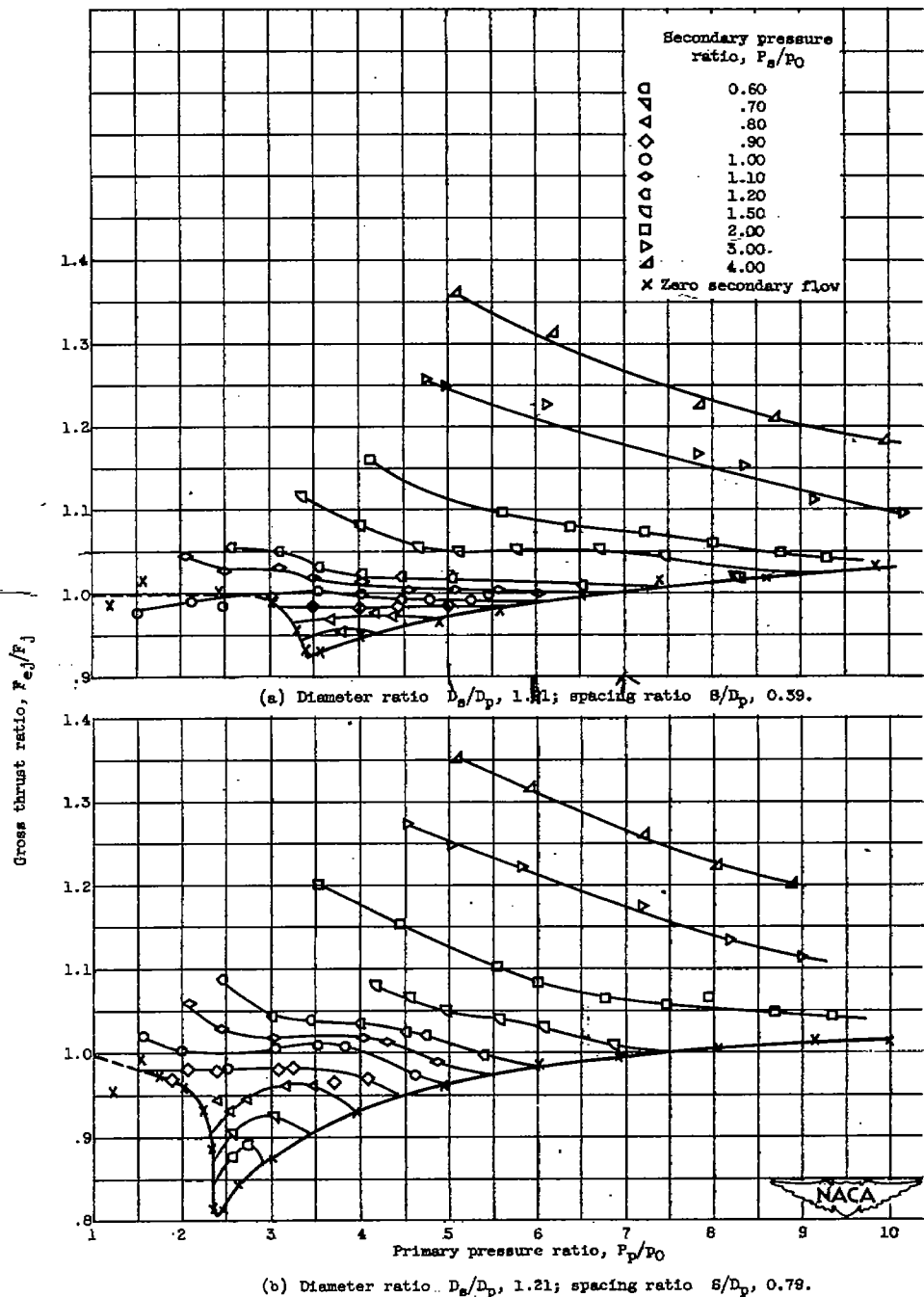
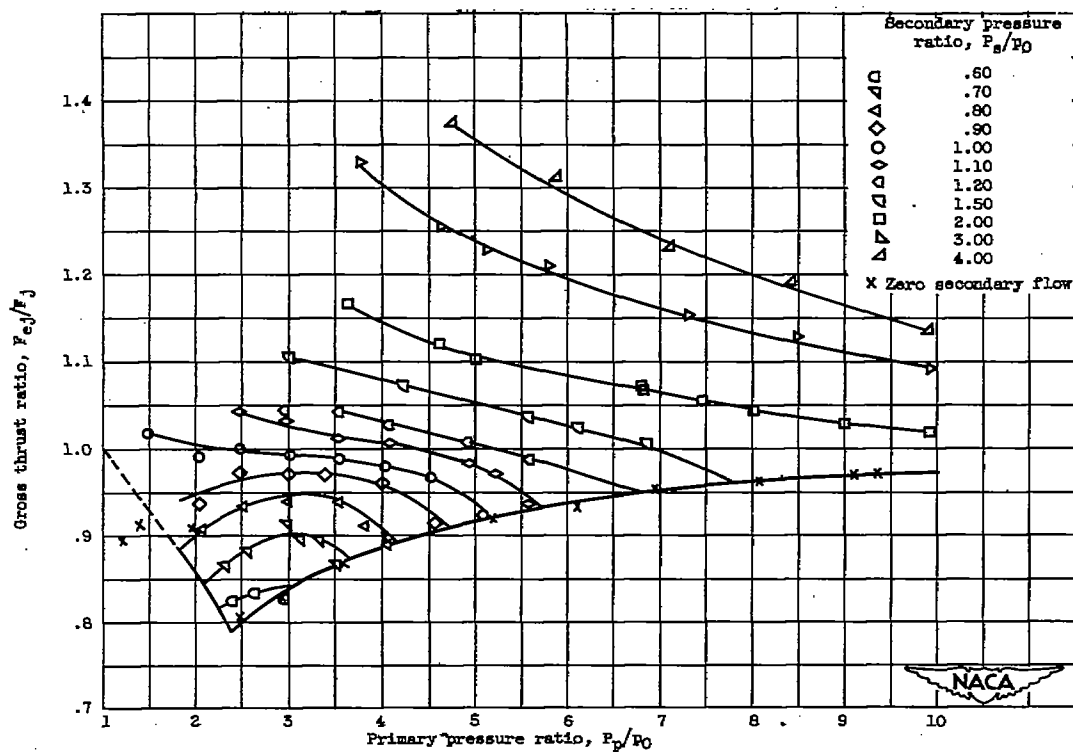


Figure 8. - Effect of primary and secondary pressure ratio on ejector gross thrust ratio.



(c) Diameter ratio D_s/D_p , 1.21; spacing ratio S/D_p , 1.18.

Figure 6. - Continued. Effect of primary and secondary pressure ratio on ejector gross thrust ratio.

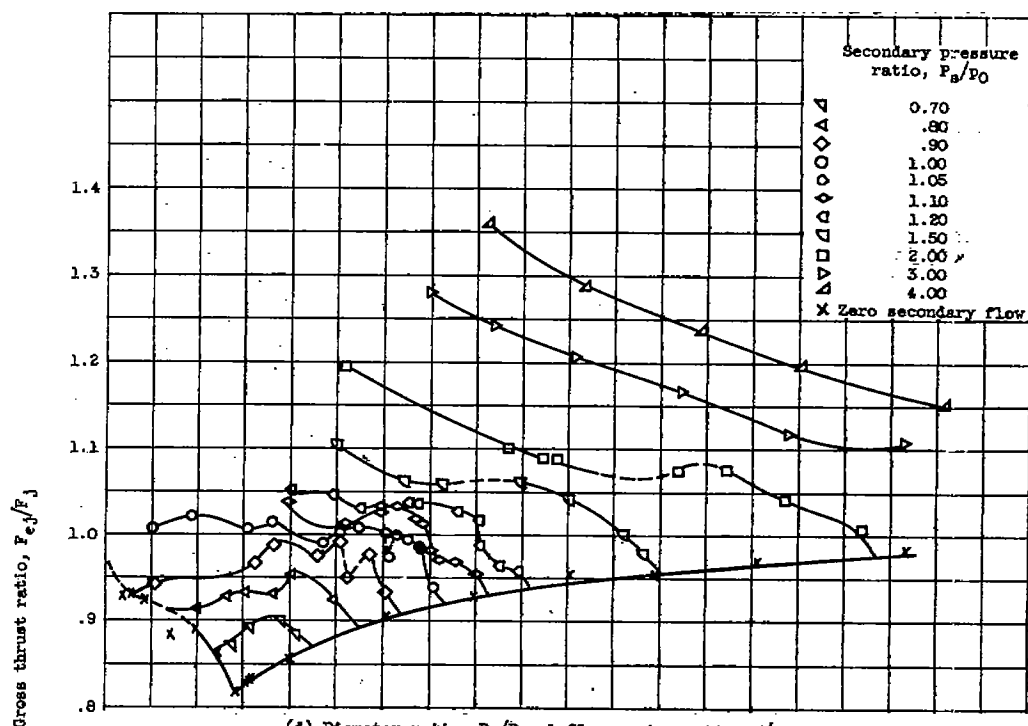
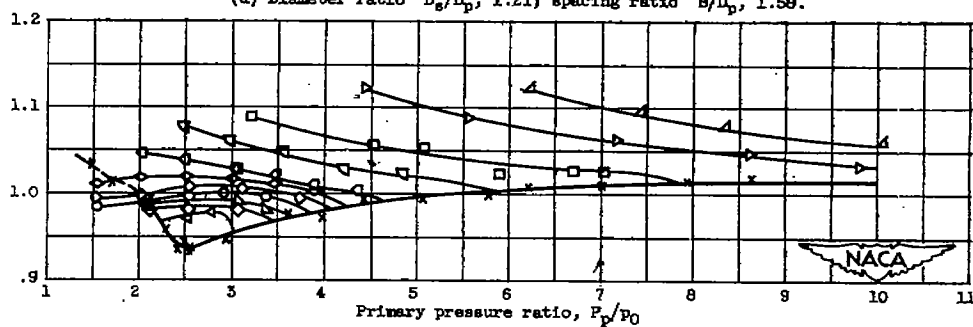
(d) Diameter ratio D_s/D_p , 1.21; spacing ratio S/D_p , 1.59.(e) Diameter ratio D_s/D_p , 1.10; spacing ratio S/D_p , 0.39.

Figure 6. - Continued. Effect of primary and secondary pressure ratio on ejector gross thrust ratio.

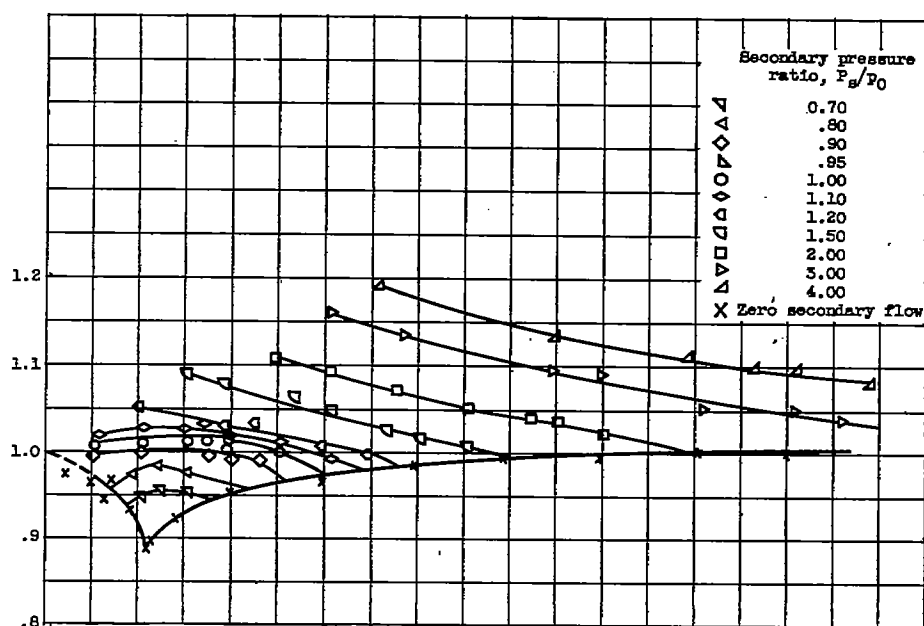
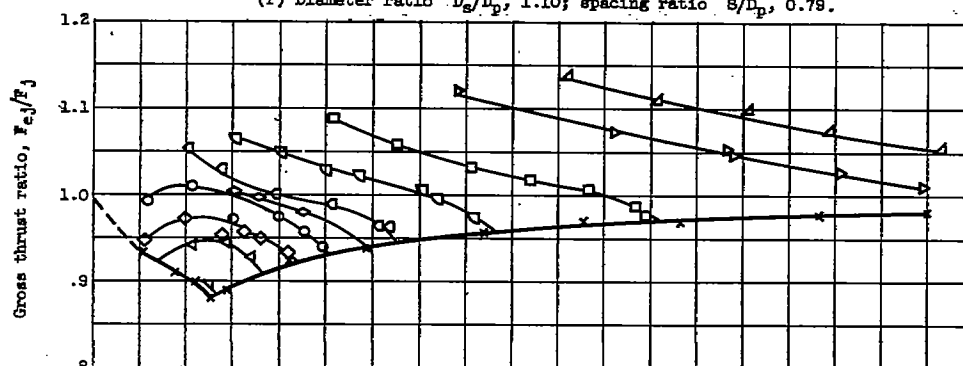
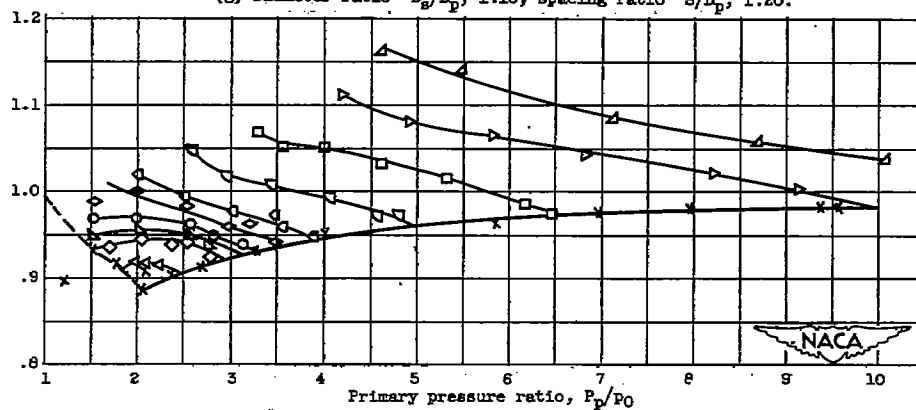
(f) Diameter ratio D_s/D_p , 1.10; spacing ratio S/D_p , 0.79.(g) Diameter ratio D_s/D_p , 1.10; spacing ratio S/D_p , 1.20.(h) Diameter ratio D_s/D_p , 1.10; spacing ratio S/D_p , 1.61.

Figure 6. - Concluded. Effect of primary and secondary pressure ratio on ejector gross thrust ratio.

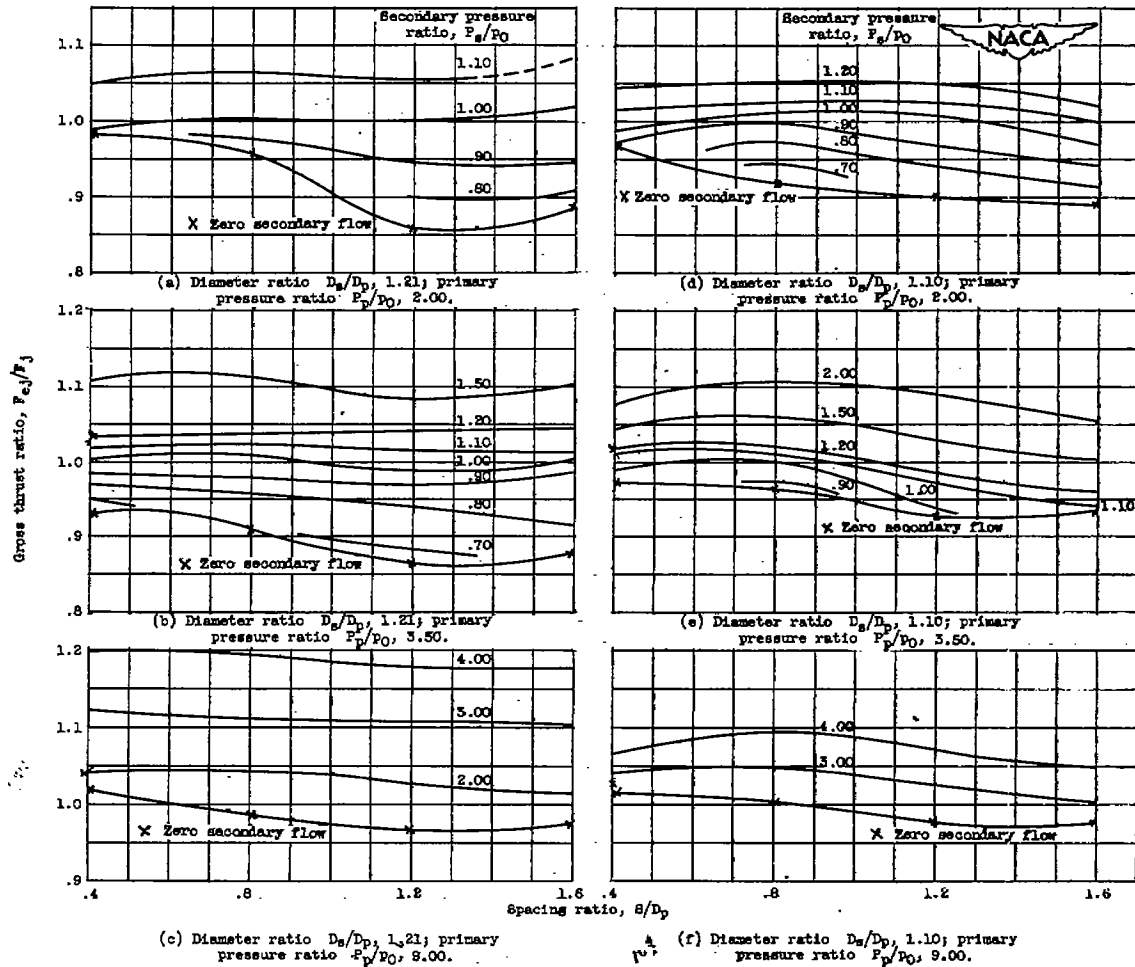
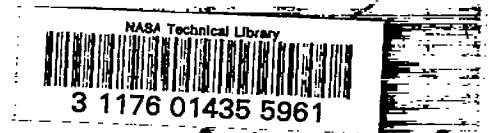


Figure 7. - Effect of spacing ratio on ejector gross thrust ratio.

SECURITY INFORMATION

[REDACTED]



[REDACTED]